JOURNAL OF VIROLOGY, Oct. 1997, p. 7781–7790 Vol. 71, No. 10
0022-538X/97/$04.00+0

In Vivo DNA Expression of Functional Brome Mosaic Virus RNA Replicons in *Saccharomyces cerevisiae*

MASAYUKI ISHIKAWA,† MICHAEL JANDA, MICHAEL A. KROL, AND PAUL AHLQUIST*

Institute for Molecular Virology, University of Wisconsin—Madison, Madison, Wisconsin 53706

Received 5 March 1997/Accepted 12 June 1997

To facilitate manipulation of brome mosaic virus (BMV) RNA replicons in *Saccharomyces cerevisiae* and for yeast genetic analysis of BMV RNA replication, gene expression, and host interactions, we constructed DNA plasmids from which BMV RNA3 and RNA3 derivatives can be transcribed in vivo from the galactose-inducible yeast *GAL1* promoter and terminated by a self-cleaving ribozyme at or near their natural 3′ ends. In galactose-induced yeast harboring such plasmids, expression of BMV RNA replication proteins 1a and 2a led to synthesis of negative-strand RNA3, amplification of positive-strand RNA3 to levels over 45-fold higher than those of DNA-derived RNA3 transcripts, and synthesis of the RNA3-encoded subgenomic mRNA for coat protein. Although the *GAL1* promoter initiated transcription from multiple sites, 1a and 2a selectively amplified RNA3 with the authentic viral 5′ end. As expected, reporter genes substituted for the 3′-proximal coat protein gene could not be translated directly from DNA-derived RNA3 transcripts, so their expression depended on 1a- and 2a-directed subgenomic mRNA synthesis. In yeast in which DNA transcription of B3CAT, an RNA3 derivative with the chloramphenicol acetyltransferase (CAT) gene replacing the coat gene, was induced, CAT activity remained near background levels in the absence of 1a and 2a but increased over 500,000-fold when 1a and 2a were expressed. Similarly, a plasmid encoding B3URA3, an RNA3 derivative with the yeast *URA3* gene replacing the coat gene, conferred uracil-independent growth to *ura3*$^-$ yeast only after 1a and 2a expression and galactose induction. Once its 1a- and 2a-dependent replication was initiated, B3URA3 was maintained in dividing yeast as a free RNA replicon, even after repression of the *GAL1* promoter or the loss of the B3URA3 cDNA plasmid. These findings should be useful for many experimental purposes.

Brome mosaic virus (BMV), a member of the alphavirus-like superfamily of positive-strand RNA viruses of animals and plants, has a genome divided among three RNAs. RNA1 and RNA2 encode the 1a and 2a proteins, respectively, which are necessary for genomic RNA replication and subgenomic mRNA synthesis (1, 21, 37). These proteins contain three domains conserved in all other members of the alphavirus-like superfamily. 1a (109 kDa) contains a C-proximal helicase-like domain and an N-proximal domain implicated in RNA capping, and 2a (94 kDa) contains a central polymerase-like domain (1, 5, 25). 1a and 2a interact with each other (35, 36) and with incompletely characterized cell factors (46, 47) to form a membrane-bound viral RNA replication complex associated with the endoplasmic reticulums of infected cells (49). BMV RNA3, a 2.1-kb RNA, encodes the 3a protein (32 kDa) and coat protein (20 kDa), which are involved in the spread of BMV infection in its natural plant hosts but are dispensable for RNA replication (2, 7, 16, 21, 42, 51). The 5′-proximal 3a gene is translated directly from RNA3. However, due to its internal location, the 3′-proximal coat gene or genes substituted for it cannot be translated directly from RNA3 (21, 31). Rather, the coat protein or its replacements are translated from a subgenomic mRNA, RNA4, which is synthesized by internal initiation on negative-strand RNA3 (Fig. 1). The RNA3 sequences required in *cis* for RNA replication and subgenomic mRNA synthesis have been mapped (19, 20).

When the yeast *Saccharomyces cerevisiae* is engineered to express BMV 1a and 2a and transfected with in vitro transcripts of appropriate RNA3 derivatives, these RNA3 derivatives undergo RNA-dependent replication and subgenomic mRNA synthesis (31). Genes introduced into such RNA3 derivatives as coat protein gene replacements are expressed in yeast in a manner completely dependent on BMV RNA replication and subgenomic mRNA synthesis and can serve as markers or reporters for these processes. Such RNA3 derivatives are passed on through mitosis to daughter cells and, when they express a selectable yeast marker gene such as the *URA3* uracil biosynthesis gene, can be maintained indefinitely in dividing yeast as persistent RNA replicons (31).

Because of the ease of growth and flexible classical and molecular genetics of yeast, this system offers avenues to analyze a number of BMV infection processes, including RNA replication and gene expression. In particular, yeast genetics may facilitate studies of virus-host interaction and host factor involvement in various infection steps. However, a possible hindrance to some uses of this system is the genetic instability of free BMV RNA replicons. In the absence of selection, such replicons are progressively lost from dividing yeast populations at a higher frequency per cell division than unselected yeast DNA plasmids (27, 31). Such losses may reflect <100% segregation of functional RNA replicons to budding daughter cells in cell division, replicon inactivation due to the high mutation and recombination frequencies associated with viral RNA replication (7, 40, 48, 53), or both. In some experiments, such as genetic screens for yeast mutants that inhibit BMV RNA replication, the genetic instability of free BMV RNA replicons would add a significant burden by increasing the background of inactivation by unwanted, replicon-associated events.

One potential solution for these problems is the development of DNA cassettes from which replicable RNA3 or RNA3

* Corresponding author. Mailing address: Institute for Molecular Virology, University of Wisconsin—Madison, 1525 Linden Dr., Madison, WI 53706-1596. Phone: (608) 263-5916. Fax: (608) 262-7414. E-mail: ahlquist@facstaff.wisc.edu.

† Present address: Department of Applied Bioscience, Hokkaido University, Sapporo 060, Japan.

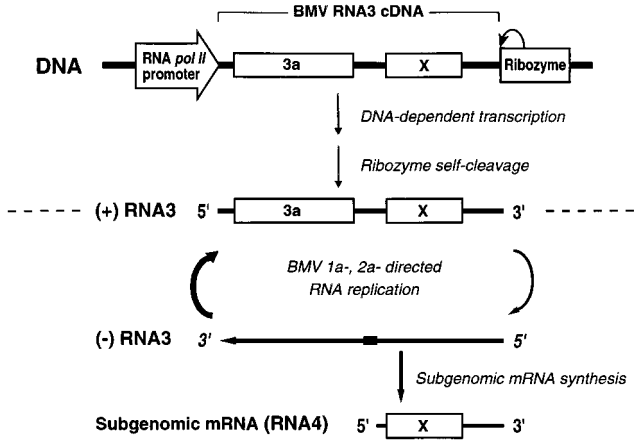

FIG. 1. Schematic diagram of a pathway for initiating BMV-specific, RNA-dependent RNA replication and subgenomic mRNA synthesis from DNA. The bracketed region at the top represents a cDNA copy of a BMV RNA3 derivative, in which single lines represent noncoding regions, the left box represents the 3a gene, and the box labeled "X" represents the BMV coat protein gene or any gene replacing it. Flanking regions represent a 5′-linked promoter and 3′-linked self-cleaving ribozyme sequence, as indicated. Steps above the dotted line are DNA-dependent steps that occur in the absence of BMV RNA replication proteins 1a and 2a. Steps below the dotted line are RNA-dependent steps that require 1a and 2a. The latter steps constitute the normal RNA replication and gene expression cycle of RNA3 in BMV infection.

derivatives could be synthesized in vivo to initiate RNA replication (Fig. 1). By providing a stable, expressible, archival DNA copy, such an "RNA-launching platform" could stabilize an RNA replicon against losses during cell division and against mutation or recombination at the RNA level. Such a DNA-based system would also facilitate the study of a wider range of viral RNA derivatives by eliminating the need for these RNAs to express a selectable marker gene. However, relative to experiments involving a single round of virus expression and/or more slowly growing cells, the need in yeast genetics to maintain RNA replication in essentially every generation and cell of a rapidly dividing population could place great demands on the efficiency of such a DNA-based system. In this paper, we describe the construction and characterization of plasmid-based DNA cassettes that inducibly transcribe RNA3 derivatives in yeast, providing efficient initiation and stable maintenance of BMV 1a- and 2a-dependent RNA replication, subgenomic mRNA synthesis, and gene expression in dividing cell populations.

MATERIALS AND METHODS

Yeast strain, cell growth, and transformation. Yeast strain YPH500 (*MAT*α *ura3-52 lys2-801 ade2-101 trp1-Δ63 his3-Δ200 leu2-Δ1*) was used throughout. Yeast cultures were grown at 30°C in defined synthetic medium containing either 2% glucose or 2% galactose (9). As appropriate, relevant amino acids were omitted to maintain selection for any DNA plasmids present and uracil was omitted to select for BMV-directed *URA3* expression. Transformation with DNA plasmids was done by the LiCl-polyethylene glycol method (29).

Plasmids and plasmid constructions. BMV 1a and 2a proteins were expressed from pB1CT19 and pB2CT15, yeast 2μm plasmids that contain the *HIS3* and *LEU2* selectable marker genes, respectively (31). All yeast plasmids described below that express BMV RNA3 derivatives were based on YCplac22, a yeast *CEN4* centromeric plasmid vector containing the *TRP1* selectable marker gene and multiple-cloning site of pUC19 (22). Standard procedures were used for all DNA manipulations (9). Where indicated below, 5′ overhanging restriction fragment ends were filled in by treatment with the Klenow fragment of DNA polymerase I and 3′ overhanging restriction fragment ends were made blunt by treatment with T4 DNA polymerase. All novel sequence junctions whose generation involved in vitro DNA polymerase reactions, including oligonucleotide-directed mutagenesis or PCR, were confirmed by DNA sequencing, and the overall structures of all plasmids were confirmed by restriction analysis. Laboratory designations for plasmids are given below in parentheses.

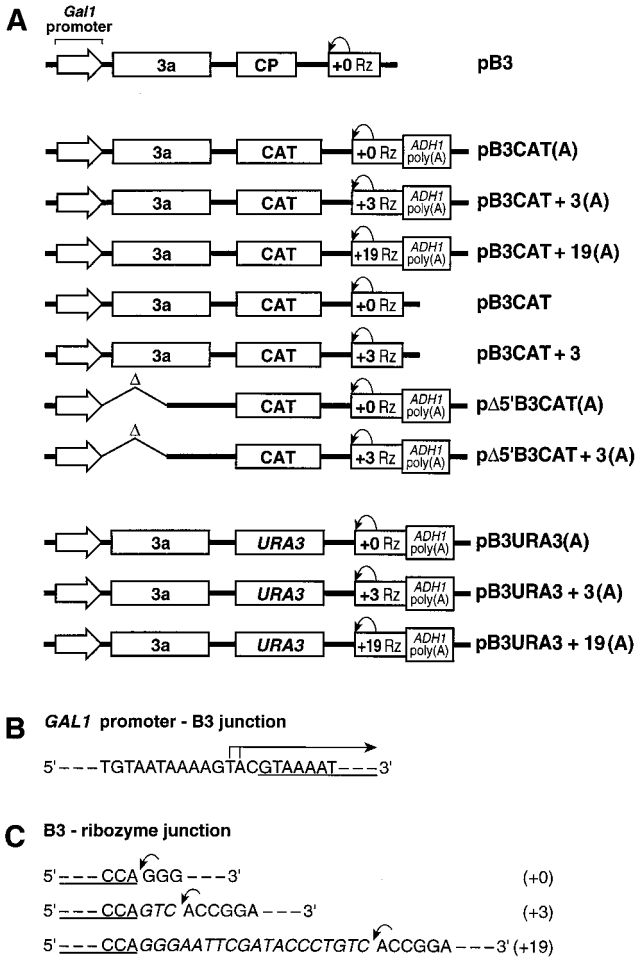

FIG. 2. Structure of plasmids used in this study. (A) Schematic of the cDNA region and flanking expression elements in plasmids carrying cDNA copies of BMV RNA3 and its B3CAT and B3URA3 derivatives. These plasmids are all based on YCplac22, a yeast centromeric plasmid vector containing the *TRP1* selectable marker gene (22) (see Materials and Methods). The open arrows at the left indicate the *GAL1* promoter, which is fused to the 5′ end of RNA3 cDNA as shown in panel B. The boxes labeled "+0 Rz," "+3 Rz," and "+19 Rz" represent self-cleaving ribozymes positioned to cleave as shown in panel C. The farthest right box in some plasmids represents the *ADH1* polyadenylation signal, as indicated. The regions between the *GAL1* promoter and ribozymes are cDNA copies of the indicated RNA3 derivatives, where single lines represent noncoding regions and the boxes labeled "3a," "CP" (coat protein), "CAT," and "*URA3*" represent the coding regions for these genes. The 0.6-kbp 5′-terminal deletion in pΔ5′B3CAT(A) and pΔ5′B3CAT+3(A) is indicated (Δ). (B) Nucleotide sequence around the junction of the *GAL1* promoter and 5′ sequence of RNA3 cDNA. The RNA3 sequence is underlined, and the bases linked to the arrow above the sequence correspond to the termination sites of the most prevalent cDNA products generated by primer extension on the *GAL1*-promoted RNA3 transcript (Fig. 4). As noted in Results, these primer extension products may reflect transcription starts at the indicated −2 and −3 positions upstream of the RNA3 sequence or a single major transcription start at the indicated A (position −2), which yields two cDNA bands due to cap-dependent incorporation of an additional nucleotide on a fraction of the cDNA. (C) Nucleotide sequences around the junctions of the 3′ sequence of RNA3 cDNA and the +0, +3, and +19 ribozymes. The RNA3 sequence is underlined, the predicted self-cleavage sites are indicated by arrows, and 3′ nonviral sequences left after self-cleavage are italicized.

(i) Intermediate plasmids. To facilitate plasmid assembly, four intermediate plasmids were first constructed. Intermediate pMII93, containing the *GAL1* promoter-RNA3 junction (Fig. 2B), was constructed by first ligating the 0.7-kbp *Hin*dIII (filled in)-*Eco*RI *GAL1* promoter fragment from pBM272 (33) and the

2.2-kbp *Pst*I (blunted)-*Hin*dIII BMV RNA3 fragment from pB3UR1 (31) between the *Eco*RI and *Hin*dIII sites of pUC119 and then deleting intervening bases between the *GAL1* promoter major start site and the 5′ end of RNA3 by the method of Kunkel et al. (39), using the 5′-phosphorylated oligonucleotide d(CAAATGTAATAAAAGTACGTAAAATACCAAC).

Intermediate pMII50, containing the RNA3-hepatitis delta virus ribozyme junction (+0-nucleotide [nt] ribozyme in Fig. 2C [ribozymes mentioned herein are named for the position at which they self-cleave 3′ of the natural 3′ end of RNA3 cDNA]) and the downstream *ADH1* polyadenylation signal, was constructed as follows. First, pB3UR5 was constructed by PCR amplifying the B3URA3 sequence from pB3UR1 (31) by using oligonucleotides corresponding to the 5′ and 3′ ends of BMV RNA3 and then ligating the resulting product between the *Sma*I sites of p(δ0,0δ) (generously provided by L. A. Ball). Like plasmid FHV2(δ0,0δ) (10), p(δ0,0δ) is a pGEM3 (Promega) derivative containing two oppositely oriented copies of the pseudoknot ribozyme from the antigenome strand of hepatitis delta virus RNA, which cleaves almost any sequence attached to the 5′ side of its cleavage site (11). The ribozymes are oriented with cleavage sites proximal and in p(δ0,0δ) are separated by an approximately 1-kb stuffer fragment bounded by *Sma*I sites that coincide with each cleavage site. pMII50 was made by ligating the 0.45-kbp *Xba*I (filled in)-*Hin*dIII fragment of pB3UR5, containing the 3′ RNA3-ribozyme junction, and the 0.45-kbp *Hin*dIII (filled in)-*Bam*HI fragment of pAAH5 (8), containing the *ADH1* polyadenylation signal, between the *Hin*dIII and *Bam*HI sites of pUC119.

Intermediate pMII62, containing the RNA3-+19-nt satellite tobacco ringspot virus ribozyme junction (Fig. 2C) and the downstream *ADH1* polyadenylation signal, was constructed by ligating the 0.3-kbp *Bam*HI (filled in)-*Hin*dIII fragment of pB3-17-self (17) (generously provided by J. Bujarski), containing the RNA3-+19 ribozyme junction, and the 0.45-kbp *Hin*dIII (filled in)-*Bam*HI fragment from pAAH5 (8), containing the *ADH1* polyadenylation signal, between the *Hin*dIII and *Bam*HI sites of pUC119.

Intermediate pMII463, containing the RNA3-+3-nt satellite tobacco ringspot virus ribozyme junction (Fig. 2C) and the downstream *ADH1* polyadenylation signal, was constructed as follows. pMII62 was cleaved at the *Bst*NI site overlapping the 3′ terminus of RNA3, the *Bst*NI ends were filled in, and then pMII62 was cleaved again at the downstream *Sal*I site between the ribozyme and the *ADH1* polyadenylation signal. The ribozyme so removed was then replaced by ligating in a new ribozyme cassette with shorter flanking regions, made by annealing four 5′-phosphorylated oligonucleotides, d(GTCACCGGATGTG TTTTCC), d(GGTCTGATGAGTCCGTGAGGACGAAACTGGAAT), d(TC GAATTCCAGTTTCGTCCTCAC), and d(GGACTCATCAGACCGGAAAA CACTCCGGTGAC); the first two oligonucleotides comprise the transcript-sense strand and the last two comprise the antisense strand.

(ii) pB3CAT+3(A) (pB3MI6) and pB3CAT+19(A) (pB3MI1). The 1.0-kbp *Eco*RI-*Afl*III fragment from pMII93 (containing the *GAL1* promoter-5′ RNA3 junction), the 1.8-kbp *Afl*III-*Hin*dIII fragment from pB3CA101 (31) (containing most of B3CAT), and the 0.7-kbp *Hin*dIII-*Bam*HI 3′ RNA3/ribozyme/polyadenylation signal fragment from pMII463 [for pB3CAT+3(A)] or pMII62 [for pB3CAT+19(A)] were cloned between the *Eco*RI and *Bam*HI sites of YCplac22 (22), a yeast centromeric plasmid vector containing the *TRP1* nutritional marker gene.

(iii) pB3CAT(A) (pB3MI7). The 0.7-kbp *Kpn*I-*Sma*I fragment from pMII50, containing the 3′ RNA3-+0-nt ribozyme junction and polyadenylation signal, was cloned between the *Bam*HI (filled-in) and *Kpn*I sites of pB3CAT+19(A).

(iv) pB3CAT (pB3MI15) and pB3CAT+3 (pB3MI14). The *ADH1* polyadenylation signal was removed by deleting the 0.45-kbp *Bam*HI-*Bam*HI fragment from pB3CAT(A) and the 0.45-kbp *Bam*HI-*Eco*RI fragment from pB3CAT+3(A), respectively.

(v) pΔ5′B3CAT(A) (pB3MI13) and pΔ5′B3CAT+3(A) (pB3MI12). The 0.6-kbp *Sna*BI-*Cla*I fragment, comprising the 5′ 600 bp of RNA3, was deleted from pB3CAT(A) and pB3CAT+3(A), respectively.

(vi) pB3 (pB3RO39). The *Cla*I-*Kpn*I region of pB3CAT, comprising the region from the middle of the 3a gene to the 3′ noncoding region of RNA3, was replaced with the 1.6-kbp *Cla*I-*Kpn*I fragment from pB3TP8 (32), which contains the corresponding sequence of wild-type RNA3.

(vii) pB3URA3(A) (pB3MI9), pB3URA3+3(A) (pB3MI8), and pB3URA3+19(A) (pB3MI3). The *Cla*I-*Kpn*I regions of pB3CAT(A), pB3CAT+3(A), and pB3CAT+19(A), respectively, were replaced with the 1.6-kbp *Cla*I-*Kpn*I fragment of B3URA3 cDNA from pB3UR1 (31).

CAT assays. Yeast strains grown on master plates containing appropriate synthetic medium with glucose (see above) were inoculated with a sterile loop into 3 ml of an appropriate synthetic glucose or galactose liquid medium and cultured to near saturation (typically, 24 h in glucose medium and 48 h in galactose medium). Cells were harvested by centrifugation, washed once with water, taken up in 0.15 ml of 0.1 M Tris-HCl (pH 7.5), and disrupted by vigorous agitation after addition of an equal volume of acid-washed glass beads. The lysate was incubated at 60°C for 10 min to inactivate potential yeast acetyltransferases (31) and centrifuged for 5 min at 12,000 × *g*. A portion of the supernatant was assayed for chloramphenicol acetyltransferase (CAT) activity by using [^{14}C]chloramphenicol (21, 31), and the resulting thin-layer chromatography plates were scanned and signals were quantitated by using a BAS1000 radioactive imaging system (Fuji Film). To stay within the linear range of the assay, yeast extracts were diluted if needed with measured volumes of 0.1 mg of bovine serum albumin per ml–0.1 M Tris-HCl (pH 7.5) until the portion assayed acetylated less than 50% of the chloramphenicol present. Protein concentrations were determined by the Bradford method (14).

RNA analysis. Extraction of total yeast RNA and Northern blot hybridization analysis were performed as described previously (31). RNA3-derived RNAs were detected with strand-specific ^{32}P-labeled RNA probes transcribed in vitro from pBCPSN1 (28), which contains the *Sac*I-*Nsi*I fragment of the BMV coat protein gene between bacteriophage T7 and T3 promoters, or pB3HE1 (20), which contains a *Hin*dIII-*Eco*RI cDNA fragment comprising the 3′-terminal 200 noncoding bases of RNA3 between bacteriophage SP6 and T7 promoters. For all quantitative analyses of Northern blots, membranes were analyzed with a model 425 PhosphorImager radioactive imaging system (Molecular Dynamics, Sunnyvale, Calif.).

Primer extensions were carried out essentially as described previously (9) by using total RNA from 7×10^7 yeast cells, 10 ng of oligonucleotide d(TAGAATGTTCGCCGG) labeled at the 5′ end with ^{32}P, and 20 U of avian myeloblastosis virus reverse transcriptase (Life Sciences) in a 45-μl reaction mixture. Each reaction mixture was incubated for 1 h at 42°C, ethanol precipitated, and resuspended in 12 μl of 90% formamide–20 mM EDTA–0.1% xylene cyanol–0.1% bromphenol blue, and 3 μl was loaded on a standard 6% acrylamide sequencing gel. For comparison, a DNA sequence ladder was prepared with the above-mentioned labeled primer, pB3 DNA template, and a Sequenase DNA sequencing kit (U.S. Biochemicals), substituting unlabeled dATP for ^{32}P-labeled dATP.

RESULTS

DNA-initiated, 1a- and 2a-dependent accumulation of RNA3 replication intermediates. To examine the feasibility of initiating RNA3 replication from DNA as in Fig. 1, we used pB3, a yeast centromeric plasmid containing a full-length BMV RNA3 cDNA (Fig. 2A). Since extra nonviral 5′ or 3′ nucleotides can substantially reduce the infectivity of BMV RNAs (2, 13, 32), the 5′ end of RNA3 cDNA was linked to the galactose-inducible, glucose-repressible yeast *GAL1* promoter, placing the major transcription initiation sites near the authentic viral 5′ end (Fig. 2B). The 3′ end of the RNA3 cDNA was linked to a well-characterized, self-cleaving ribozyme from the antigenome of hepatitis delta virus RNA (11), with the cleavage site positioned to produce the authentic viral 3′ end (+0 end [Fig. 2C]).

pB3 was transformed into strain YPH500 yeast having or lacking plasmids expressing BMV RNA replication proteins 1a and 2a (hereafter referred to as 1a2a$^+$ and 1a2a$^-$ yeast strains). The 1a and 2a mRNAs produced by these expression plasmids lack 5′- and 3′-terminal *cis*-acting RNA replication signals of BMV RNA1 and RNA2 (31) and consequently are not substrates for BMV RNA replication. After initial growth in glucose-containing medium, 1a2a$^+$ and 1a2a$^-$ yeasts with pB3 were transferred to medium containing galactose to induce RNA3 transcription from the *GAL1* promoter. Total RNA samples were isolated at intervals and analyzed by Northern blotting with strand-specific probes for positive- and negative-strand RNA3 (Fig. 3). To compare the RNA3 levels per cell at various times postinduction (p.i.) in these dividing cell cultures, equal amounts of total yeast RNA were loaded for each sample. At 0 h p.i., no discrete bands were detected with probes for positive- or negative-strand RNA3 sequences. Consistent with the reported 3- to 5-h lag for relief of glucose repression and *GAL1* promoter induction (34), a positive-sense band that comigrated with wild-type BMV RNA3 appeared in 6-h-p.i. RNA samples from 1a2a$^-$ or 1a2a$^+$ yeast with pB3 (Fig. 3A). In 1a2a$^-$ yeast, this band peaked by 24 h p.i. and then stabilized or declined as the culture reached saturation.

In 1a2a$^+$ yeast, positive-strand RNA3 levels increased much more dramatically (Fig. 3A) and by 48 h p.i. were 12- to 15-fold higher than in 1a2a$^-$ yeast (based on PhosphorImager measurements of the blot in Fig. 3A and similar Northern blots). When such yeast cultures were passaged to new galactose medium to allow continued growth, RNA3 levels remained

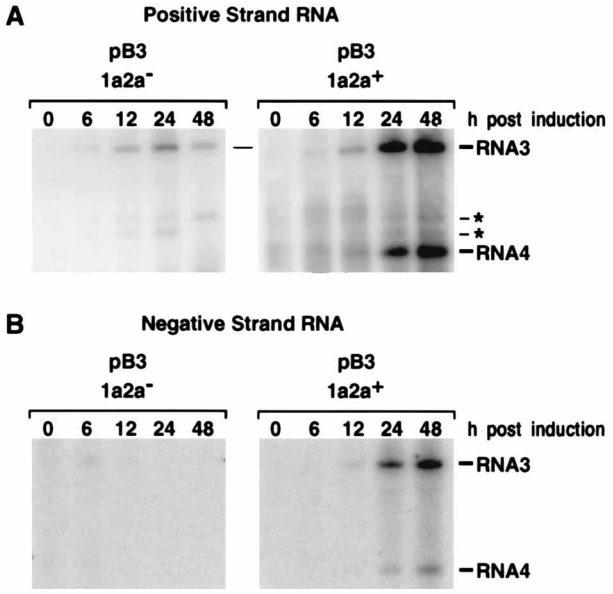

FIG. 3. Time course of galactose induction of DNA-dependent transcripts from wild-type BMV RNA3 cDNA fused to the *GAL1* promoter and subsequent RNA-dependent RNA3 amplification and RNA4 transcription in the presence of BMV RNA replication proteins 1a and 2a. 1a2a$^+$ and 1a2a$^-$ yeast strains containing pB3 were precultured in glucose-containing liquid medium, washed with water, and transferred to galactose-containing liquid medium. After 0, 6, 12, 24, and 48 h of culture in galactose medium, equal portions of the culture were harvested and total RNA was prepared, denatured by glyoxylation, fractionated in a 0.8% agarose gel, and analyzed by Northern blot hybridization. Equal amounts of total RNA were loaded per lane. (A) RNA3-derived positive-strand RNAs were detected with a ^{32}P-labeled RNA probe complementary to coding sequences in the coat protein gene. Asterisks indicate two minor bands discussed in Results. (B) RNA3-derived negative-strand RNAs were detected with a ^{32}P-labeled RNA probe corresponding to coding sequences in the coat protein gene. Note that the blot image shown represents an exposure approximately 10 times longer than that of panel A, since the accumulation of negative-strand RNA3 in these yeasts is 20- to 100-fold less than that of positive-strand RNA3 (see Results).

constant in 1a2a$^-$ cells but continued to increase in 1a2a$^+$ cells. After one or two additional such passages, positive-strand RNA3 in 1a2a$^+$ yeast reached steady-state levels 47-fold higher than in 1a2a$^-$ yeast (averaged over six independent experiments; standard deviation, ±4-fold).

In 1a2a$^+$ but not 1a2a$^-$ yeast bearing pB3, a band that comigrated with the BMV subgenomic coat protein mRNA, RNA4, appeared between 6 and 12 h p.i. and by 48 h had increased to 60% of the level of RNA3 (Fig. 3A). At later times two weak bands were visible above RNA4 (Fig. 3A). These bands were present in RNA samples from 1a2a$^-$ as well as 1a2a$^+$ yeast and may represent RNA3 degradation products.

No consistent negative-strand RNA3-related bands were visible at any time in 1a2a$^-$ yeast with pB3 (Fig. 3B). For 1a2a$^+$ yeast with pB3, a band comigrating with negative-strand RNA3 appeared between 6 and 12 h p.i. and increased through 48 h p.i. By 24 h, a band comigrating with negative-strand RNA4 also appeared. In contrast to the more nearly equal accumulations of positive-strand RNA3 and RNA4, by 48 h levels of negative-strand RNA4 were only 20% of those of negative-strand RNA3. Negative-strand RNA4 also accumulates much more slowly than negative-strand RNA3 in BMV-infected plant protoplasts (38).

In nondividing, BMV-infected barley protoplasts, negative-strand RNA accumulation ceases 6 to 8 h after inoculation while positive-strand RNA synthesis continues, yielding a 100:1 excess of positive- to negative-strand RNA3 by 24 to 48 h after inoculation (19, 38). Side-by-side comparisons of protoplast and yeast RNA samples on positive- and negative-strand RNA blots such as those in Fig. 3 showed that the ratio of positive- to negative-strand RNA3 in pB3-containing, 1a2a$^+$ yeast at 48 h p.i. was about fivefold less than in protoplasts, i.e., 20:1. As noted above, further growth of pB3-containing, 1a2a$^+$ yeast leads to a three- to fourfold increase in positive-strand RNA3, shifting this ratio toward that of late-stage-infected barley cells. Slower development of asymmetry of positive- and negative-strand RNA in yeast may reflect yeast cell division every 2 to 4 h and consequent reinitiation of negative-strand synthesis in new daughter cells.

Selective amplification of RNA3 species with natural viral 5′ ends. The 5′ ends of RNA3 species in pB3-containing 1a2a$^-$ and 1a2a$^+$ yeast strains were examined by primer extension with reverse transcriptase (Fig. 4). As previously established, BMV virion RNA from infected plants (Fig. 4, lane 1) yielded two bands; the lower band corresponded to the 5′ end of RNA3, while the upper, intense band resulted from cap-dependent incorporation of an additional nucleotide (3). Similar cap-dependent incorporation of an additional nucleotide has been seen for other capped RNAs (6, 23). Consistent with reported multiple *GAL1* transcription starts (33), galactose-

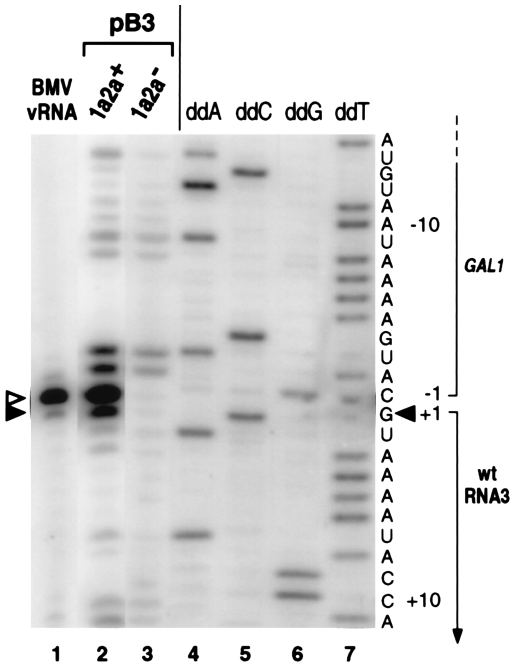

FIG. 4. Primer extension analysis of the 5′ ends of RNA3 species present in pB3-containing 1a2a$^+$ and 1a2a$^-$ yeasts after 48 h of growth in galactose-containing liquid medium. An oligodeoxyoligonucleotide labeled at the 5′ end with ^{32}P and complementary to bases 30 to 44 of BMV RNA3 was annealed with BMV virion RNA (vRNA) from infected barley plants or total RNA from 1a2a$^+$ or 1a2a$^-$ yeast harboring pB3, the primer was extended with reverse transcriptase, and the resulting cDNA products were electrophoresed in a 6% polyacrylamide sequencing gel and autoradiographed. A dideoxynucleotide sequencing ladder prepared by extending the same 5′-end-labeled primer on pB3 plasmid DNA was coelectrophoresed (lanes 4 to 7). The sequence corresponding to the sense of the RNA product is shown at right, with sequences derived from the *GAL1* promoter and RNA3 cDNA indicated by brackets and numbered relative to the 5′ terminus of wild-type (wt) BMV RNA3. The closed arrowheads indicate the primer extension band corresponding to the first nucleotide of natural RNA3, and the open arrowhead indicates the band corresponding to cap-dependent incorporation of an additional nucleotide (see Results).

induced 1a2a$^-$ yeast harboring pB3 contained RNA3 species with multiple 5′ ends (Fig. 4, lane 3). The most prominent bands were doublets at positions −2/−3 and −8/−9 relative to the 5′ end of natural RNA3 (Fig. 4, lanes 4 to 7). These doublets may primarily represent transcription starts at −2 and −8, each with a higher band from cap-dependent incorporation (see above). Weaker bands at positions −1 to +3 and −10 to −14 may reflect additional transcription starts. Neither the major nor minor RNA species were detected with RNA from pB3-containing yeast grown in glucose medium, in which transcription from the *GAL1* promoter is repressed to undetectable levels (34) (data not shown).

Galactose-induced 1a2a$^+$ yeast with pB3 contained the same RNA3 species as 1a2a$^-$ yeast with pB3, plus an intense pair of bands at +1/−1, corresponding to the 5′ end of natural BMV RNA3 (Fig. 4, lane 2). This suggested that either 1a and 2a specifically amplified a small starting population of transcripts with the natural 5′ end or replication started with longer transcripts that quickly lost any extra nucleotides during 1a- and 2a-directed amplification. In some experiments, the bands at −2/−3 appeared slightly increased in 1a2a$^+$ yeast relative to upper bands and so may have contributed to initiating RNA3 replication.

Induction of 1a- and 2a-dependent CAT expression from DNA. B3CAT is an RNA3 derivative with the coat protein gene replaced by the CAT gene (Fig. 2A). B3CAT in vitro transcripts transfected into plant cells or yeast express CAT only if the recipient cells contain 1a and 2a to replicate B3CAT RNA and synthesize subgenomic CAT mRNA (21, 31). To test whether 1a- and 2a-dependent CAT expression could be initiated in vivo from DNA, we constructed pB3CAT(A), pB3CAT+3(A), and pB3CAT+19(A) (Fig. 2A). These yeast centromeric plasmids contain B3CAT cDNA between the upstream *GAL1* promoter and a downstream ribozyme and differ only in their ribozymes. pB3CAT(A) contains the hepatitis delta virus ribozyme (11), positioned to cleave at the natural RNA3 3′ end as in pB3 (Fig. 2C). pB3CAT+3(A) and pB3CAT+19(A) contain a satellite tobacco ringspot virus ribozyme (24), positioned to cleave 3 and 19 nt, respectively, after the RNA3 3′ end (Fig. 2C).

CAT expression from these plasmids was highly dependent on 1a and 2a (Fig. 5). When grown in galactose medium to induce B3CAT transcription, 1a2a$^-$ yeast with pB3CAT(A), pB3CAT+3(A), or pB3CAT+19(A) yielded only 0.01 to 0.04 U of CAT activity/mg of total yeast protein. By contrast, galactose-grown 1a2a$^+$ yeast with pB3CAT(A) and pB3CAT+3(A) consistently yielded 50,000- to 200,000-fold-higher CAT expression (2,000 U/mg of yeast protein). CAT expression in galactose-induced 1a2a$^+$ yeast with pB3CAT+19(A) was 50-fold lower (40 U/mg of yeast protein), but this still represented a 1,000-fold increase over expression in 1a2a$^-$ yeast with pB3CAT+19(A). This reduced activity of pB3CAT+19(A) did not reflect inefficient ribozyme cleavage, since accumulation of self-cleaved transcripts from pB3CAT+19(A) in 1a2a$^-$ yeast was similar to that for pB3CAT+3(A) (results not shown).

When yeast strains carrying pB3CAT(A), pB3CAT+3(A), and pB3CAT+19(A) were grown in glucose medium to repress B3CAT transcription, CAT expression levels were low and independent of 1a and 2a (Fig. 5). Interestingly, CAT levels in glucose (0.4 to 1.6 U/mg of yeast protein) were markedly lower than for galactose-induced B3CAT transcription in 1a2a$^+$ yeast (40 to 2,000 U/mg of protein) but higher than for galactose-induced B3CAT transcription in 1a2a$^-$ yeast (0.01 to 0.04 U/mg of protein) (Fig. 2). Possible reasons for this difference are considered in Discussion.

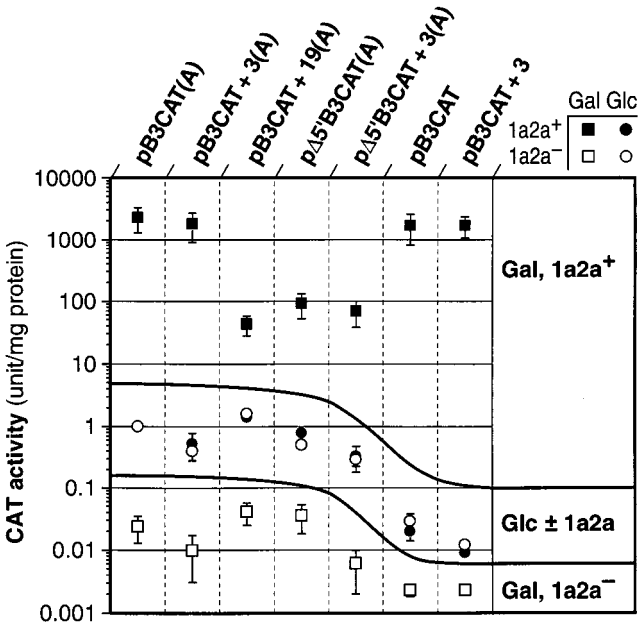

FIG. 5. CAT expression in yeast containing the B3CAT cDNA plasmids shown at the top (for plasmid structures, see Fig. 2A). To obtain equivalent final culture densities, 1a2a$^+$ (solid symbols) or 1a2a$^-$ (open symbols) yeast strains with the indicated plasmids were cultured in galactose (Gal)-containing medium for 48 h or in glucose (Glc)-containing medium for 24 h. The yeast cells then were extracted, and the CAT activities and protein concentrations of the extracts were measured as described in Materials and Methods. For each set of conditions, four independent yeast transformants were analyzed. The resulting average values were plotted on the indicated logarithmic scale, with error bars showing the standard deviations.

Effect of 5′ RNA3 sequences on DNA-initiated B3CAT expression. In keeping with the Fig. 1 pathway, 1a- and 2a-directed CAT expression from B3CAT in vitro transcripts transfected into yeast requires *cis*-acting signals for negative-strand RNA3 and subgenomic mRNA synthesis (31). However, in the plasmid-based experiments described above, it was unclear whether the template capacity of the negative-strand RNA3 synthesis pathway was saturated by DNA-derived B3CAT transcripts or whether high-level CAT expression in 1a2a$^+$ galactose-grown yeast also depended on BMV-directed amplification of positive-strand B3CAT RNA.

To test whether CAT expression might be independent of RNA-templated synthesis of positive-strand B3CAT RNA, we modified pB3CAT(A) and pB3CAT+3(A) by deleting the 5′ 600 bases of RNA3. This deletion includes 5′ noncoding sequences required for positive-strand RNA3 synthesis (1, 19, 44) but not for synthesis of negative-strand RNA3 or subgenomic mRNA (45). This deletion also removes part of the 3a gene, but mutation or deletion of the 3a gene does not affect RNA3 replication in yeast (27). The resulting plasmids, pΔ5′B3CAT(A) and pΔ5′B3CAT+3(A) (Fig. 2A), directed expression of 70 to 90 U of CAT/mg of protein in galactose-grown 1a2a$^+$ yeast (Fig. 5). Since this is 2,500- to 10,000-fold higher than the CAT expression directed by these plasmids in galactose-grown 1a2a$^-$ yeast, the *GAL1*-promoted transcripts from these plasmids must serve as templates for synthesis of negative-strand RNA that in turn synthesizes subgenomic CAT mRNA. At the same time, CAT expression directed by pΔ5′B3CAT(A) and pΔ5′B3CAT+3(A) in galactose-grown 1a2a$^+$ yeast was 10- to 20-fold lower than that directed by their parental plasmids (Fig. 5). This implied that, for pB3CAT(A)

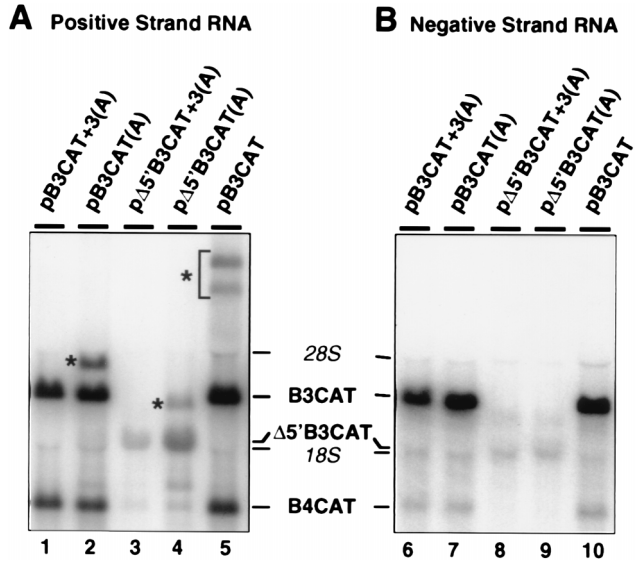

FIG. 6. Northern blot analysis of B3CAT-related RNAs in 1a2a$^+$ yeast containing the B3CAT cDNA plasmids shown at the top (for plasmid structures, see Fig. 2A). The indicated yeast strains were cultured in galactose-containing medium for 48 h, and total RNA was prepared, glyoxylated, fractionated in a 1% agarose gel, and analyzed by Northern blot hybridization. RNA3-derived positive- and negative-strand RNAs were detected with ^{32}P-labeled RNA probes complementary to or corresponding to the 3′ 200 bases of RNA3, respectively. Asterisks mark bands corresponding to *GAL1* promoter-driven transcripts that did not self-cleave at the hepatitis delta virus ribozyme cleavage site (see Results). The positions of B3CAT, Δ5′B3CAT, and subgenomic B4CAT RNAs are indicated. The leading edges of the 18S and 28S rRNA bands are also indicated, because the high RNA concentration in these bands tends to sweep nearby probe-reactive RNAs or background smear ahead of them. Most noticeably, in panel B, the 18S rRNA band overlaps the Δ5′B3CAT band. This causes some broadening of the Δ5′B3CAT signals in lanes 8 and 9 and, by similarly sweeping the background from the much more intense signals in lanes 6, 7, and 10, creates background bands comigrating with the front of the 18S/Δ5′B3CAT signal. To a lesser degree, similar effects are seen in panel A.

and pB3CAT+3(A), RNA-dependent amplification of positive-strand B3CAT RNA amplified CAT expression, presumably by enhancing synthesis of the negative-strand RNA from which subgenomic CAT mRNA is synthesized.

Northern blot analysis of total RNA from galactose-grown 1a2a$^+$ yeast bearing these plasmids was consistent with the CAT expression results (Fig. 6). In keeping with their similar levels of CAT expression, pB3CAT(A) and pB3CAT+3(A) induced similar levels of positive- and negative-strand B3CAT RNA and subgenomic CAT mRNA. Also in keeping with CAT expression results, deletion of the 5′ RNA3 sequences in pΔ5′B3CAT(A) and pΔ5′B3CAT+3(A) allowed synthesis and accumulation of negative-strand RNA3 and positive-strand subgenomic CAT mRNA, but at reduced levels. Relative to the levels induced by pB3CAT(A) and pB3CAT+3(A), positive-strand RNA3 accumulation was reduced 5- to 10-fold and subgenomic CAT mRNA accumulation was reduced 8- to 12-fold (Fig. 6A, lanes 3 and 4). Negative-strand RNA3 accumulation was also reduced approximately 10-fold (Fig. 6B, lanes 8 and 9). Though weak relative to those for the other plasmids, the negative-strand RNA3 bands seen for pΔ5′B3CAT(A) and pΔ5′B3CAT+3(A) clearly resulted from 1a- and 2a-dependent RNA synthesis, since parallel Northern analysis for negative-strand RNA in galactose-grown 1a2a$^-$ yeast with pΔ5′B3CAT (A), pΔ5′B3CAT+3(A), or any other B3CAT plasmids produced completely blank lanes even after much longer exposures than that used for Fig. 6B.

For pB3CAT(A) and pΔ5′B3CAT(A), which contain the hepatitis delta virus ribozyme, Northern blots probed for RNA3-derived positive strands showed an additional, weaker band above full-length B3CAT or Δ5′B3CAT RNA (Fig. 6A, lanes 2 and 4). Several results suggest that these bands represent a fraction of *GAL1*-promoted pB3CAT transcripts that terminate at a downstream *ADH1* polyadenylation site (Fig. 2A) but fail to undergo ribozyme self-cleavage. First, these bands are present only in galactose-grown yeast and their migration relative to B3CAT and Δ5′B3CAT RNAs is consistent with the 480-nt interval between the ribozyme cleavage site and *ADH1* polyadenylation site and the average 60-nt length of yeast poly(A) (52). Second, these bands are present at similar levels in 1a2a$^-$ and 1a2a$^+$ yeasts. Third, when the *ADH1* polyadenylation signal is deleted from pB3CAT(A), the band in question disappears and is replaced by two new bands much higher on the gel, consistent with downstream termination of uncleaved primary transcripts at or near the next polyadenylation site on the plasmid (following the *TRP1* marker gene) and the replication origin/centromere region (Fig. 6A, lane 5; see also next section). The absence of an analogous extra band from pB3CAT+3(A) or pΔ5′B3CAT+3(A) implies that, in yeast, either the satellite tobacco ringspot virus ribozyme self-cleaves more efficiently than the hepatitis delta virus ribozyme or the uncleaved primary transcripts are unstable.

Effect of downstream polyadenylation signal on background CAT expression. pB3CAT(A), pB3CAT+3(A), and pB3CAT+19(A) contain the *ADH1* polyadenylation signal downstream of their ribozymes (Fig. 2A). Addition of a polyadenylation signal was tested because polyadenylation has been implicated in facilitating export of RNA polymerase II transcripts from the nucleus to the cytoplasm (18, 26). For comparison, pB3CAT and pB3CAT+3 were derived from pB3CAT(A) and pB3 CAT+3(A), respectively, by deleting the *ADH1* polyadenylation signal (Fig. 2A). As shown in Fig. 5, removal of this polyadenylation signal had no effect on the high levels of BMV-directed CAT expression by galactose-grown 1a2a$^+$ yeast. Similarly, Northern blotting revealed that pB3CAT produced levels of positive- and negative-strand B3CAT RNA and subgenomic CAT mRNA equal to those of pB3CAT(A) and pB3CAT+3(A) (Fig. 6, lanes 5 and 10). However, for pB3CAT and pB3CAT+3 in glucose medium where B3CAT transcription was repressed, 1a- and 2a-independent background levels of CAT expression were reduced 40- to 50-fold relative to those for pB3CAT(A) and pB3CAT+3(A) (Fig. 5). Moreover, for galactose-grown 1a2a$^-$ yeast, CAT expression from pB3CAT or pB3CAT+3 was 5- to 10-fold lower than from pB3CAT(A) or pB3CAT+3(A) (Fig. 5). Due to this reduced background, CAT expression for pB3CAT or pB3CAT+3 in galactose medium was over 500,000-fold higher in 1a2a$^+$ than 1a2a$^-$ yeast (Fig. 5).

DNA-based induction of BMV-dependent, uracil-independent growth. To use the yeast *URA3* gene as the basis of a colony-selectable, 1a- and 2a-dependent, DNA-generated phenotype, we constructed pB3URA3(A), pB3URA3+3(A), and pB3URA3+19(A) (Fig. 2A). These plasmids were constructed in parallel to pB3CAT(A), pB3CAT+3(A), and pB3CAT+19 (A), respectively, and have the same structures except that *URA3* was substituted for the CAT gene.

YPH500 yeast contains an inactivating insertion in the chromosomal *URA3* uracil biosynthesis gene (50) and thus is unable to grow without uracil (Fig. 7A, row 9). However, 1a2a$^+$ YPH500 yeast with pB3URA3(A) or pB3URA3+3(A) formed colonies on galactose medium lacking uracil (Fig. 7A, rows 3 and 5). The growth rate of these colonies in the absence of uracil was equal to or slightly higher than that of 1a2a$^+$

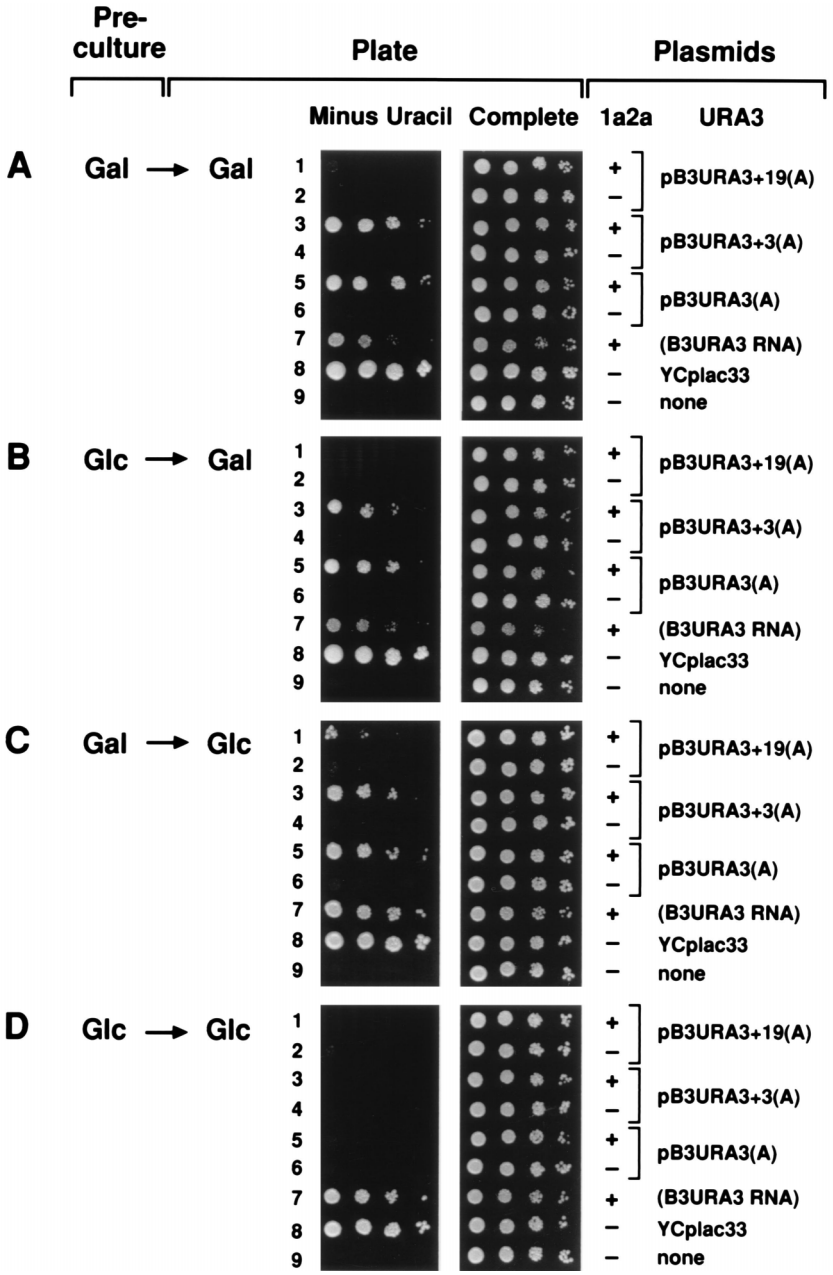

FIG. 7. Tests of B3URA3 plasmids for the ability to support 1a- and 2a-dependent, uracil-independent growth by *ura3-52* yeast. As shown at the right, 1a2a$^+$ or 1a2a$^-$ yeast strains harbored the indicated B3URA3 plasmids (see Fig. 2A for plasmid structures), constitutively *URA3*-expressing plasmid YCplac33 (22), or the free B3URA3 RNA replicon. Each strain was precultured in defined liquid medium containing galactose (Gal) or glucose (Glc), as indicated at the left, for a time sufficient to approach saturation (24 h for glucose and 48 h for galactose). For each strain, the appropriate amino acids were omitted from the preculture medium to maintain selection for all plasmids present (see Materials and Methods). After being precultured, the cells were harvested, washed with sterile water, and diluted to A_{600}s of 0.2, 0.025, 0.003, and 0.0004 (8-fold serial dilutions). Two microliters of each dilution was spotted onto plates of defined synthetic medium containing galactose or glucose and lacking or containing uracil, as indicated. The serial dilution series corresponds to plating approximately 10 to 20 cells in the most dilute spot for each strain. For colony formation, plates with galactose medium lacking uracil, complete galactose medium, glucose medium lacking uracil, and complete glucose medium were incubated at 30°C for 5, 4, 3, and 2 days, respectively, and photographed.

YPH500 harboring B3URA3 RNA as a free RNA replicon (Fig. 7A, row 7). All three of these strains grew slightly more slowly than 1a2a$^-$ YPH500 in which *URA3* was expressed from yeast centromeric plasmid YCplac33 (Fig. 7A, row 8) (22), but the persistence of this growth difference in the presence of uracil (Fig. 7A, complete medium) and other experience show that it reflects an effect of 1a and 2a expression rather than uracil selection. Northern blot analysis of galactose-grown 1a2a$^+$ yeast with pB3URA3(A) or pB3URA3+3(A) confirmed the presence of B3URA3 RNA and the expected subgenomic RNA at levels equal to those previously documented for yeast with B3URA3 RNA as a free replicon (31).

1a2a$^-$ yeast with pB3URA3(A) or pB3URA3+3(A) did not grow on galactose medium without uracil (Fig. 7A, rows 4 and 6). Thus, *URA3* expression from these plasmids depended on 1a and 2a, and though B3CAT results suggested that the poly-

adenylation signal in pB3URA3(A) and pB3URA3+3(A) may increase 1a- and 2a-independent background expression of *URA3*, any such background expression was insufficient for uracil-independent growth. As expected, *URA3* expression from pB3URA3(A) or pB3URA3+3(A) also depended on galactose-induced DNA transcription (Fig. 7D, rows 3 and 5; see also next section). However, as long as galactose was included in the plating media, preculturing such yeast in galactose rather than glucose provided only a modest increase in plating efficiency in the absence of uracil (Fig. 7A and B, rows 3 and 5).

In Fig. 7A, after preculture in galactose, the plating efficiencies of 1a2a$^+$ yeast with pB3URA3(A) or pB3URA3+3(A) on galactose medium without uracil were slightly lower than on complete galactose medium (rows 3 and 5). However, to support the growth of control strains lacking one or more BMV plasmids (Fig. 7A, rows 2, 4, and 6 to 9), the plates contained histidine, leucine, and tryptophan, which must be omitted to select for corresponding marker genes on the 1a and 2a expression plasmids and pB3URA3 plasmids, respectively (see Materials and Methods). When these three amino acids were omitted from the plates to maintain plasmid selection, the plating efficiency of 1a2a$^+$ yeast with pB3URA3(A) or pB3URA3+3(A) on galactose medium without uracil was identical to that on galactose medium with uracil (data not shown). Thus, *URA3* expression was induced in all cells retaining the complete set of BMV plasmids.

Derivation of free RNA replicon B3URA3 from DNA. To see if plasmid-launched B3URA3 RNA could be maintained in yeast as a free cytoplasmic RNA replicon after the *GAL1* promoter was repressed with glucose, 1a2a$^+$ yeast strains with pB3URA3(A) or pB3URA3+3(A) were precultured in liquid galactose medium for 48 h and then plated on solid glucose medium lacking uracil. With either plasmid, Ura$^+$ colonies appeared (Fig. 7C, rows 3 and 5) that grew as rapidly as 1a2a$^+$ YPH500 harboring B3URA3 RNA as a free RNA replicon (row 7). Northern blotting as in Fig. 3 showed that, despite repression of B3URA3 cDNA transcription, these colonies contained the expected B3URA3 RNA and subgenomic URA3 mRNA species, and primer extension as in Fig. 4 showed that the 5′ end of the B3URA3 RNA was identical to that of natural RNA3 rather than the spectrum of 5′ ends produced by *GAL1*-promoted DNA transcription (results not shown). To confirm that maintenance of these RNAs and the Ura$^+$ phenotype was independent of pB3URA3(A) or pB3URA3+3(A), the yeast strains were cultured without selection for the *TRP1* nutritional marker on these plasmids, Ura$^+$ cell lines in which the relevant pB3URA3 plasmid had been lost were isolated (confirmed by Southern blotting), and the continued maintenance of the B3URA3 and subgenomic mRNA species was verified by Northern blotting.

As expected, 1a and 2a expression and initial *GAL1* transcription were required to establish the plasmid-independent Ura$^+$ state. No Ura$^+$ colonies formed from galactose-precultured 1a2a$^-$ yeast with pB3URA3(A) or pB3URA3+3(A) (Fig. 7C, rows 4 and 6) or when 1a2a$^+$ yeast strains with pB3URA3(A) or pB3URA3+3(A) were precultured in liquid medium containing glucose to repress the *GAL1* promoter (plus uracil to allow growth) and then plated on glucose medium lacking uracil (Fig. 7D, rows 3 and 5).

In parallel with the 50-fold-lower CAT expression from pB3CAT+19(A) (Fig. 5), pB3URA3+19(A) did not support uracil-independent growth of 1a2a$^+$ yeast on galactose medium lacking uracil (Fig. 7A and B, rows 1). However, when 1a2a$^+$ yeast bearing pB3URA3+19(A) was precultured in galactose medium with uracil and then plated on glucose medium lacking uracil, a few colonies appeared, with a plating efficiency about 50-fold less than that of 1a2a$^+$ yeast with pB3URA3(A) or pB3URA3+3(A) under the same conditions (Fig. 7C, row 1). These pB3URA3+19(A)-derived colonies grew as rapidly in the absence of uracil as the other Ura$^+$ cells tested and contained B3URA3 and subgenomic URA3 mRNA species that were maintained along with the Ura$^+$ phenotype after the yeast was cured of pB3URA3+19(A). Thus, pB3URA3+19(A) transcripts can initiate B3URA3 RNA replication at a low frequency. The failure of 1a2a$^+$ pB3URA3+19(A)-containing yeast to yield any Ura$^+$ colonies on galactose medium is considered in Discussion.

DISCUSSION

This paper describes an effective, DNA-based, in vivo inoculation system to initiate and maintain BMV 1a- and 2a-dependent RNA replication and gene expression in yeast. In this system, DNA-generated transcripts of BMV RNA3 derivatives initiated de novo RNA replication at a frequency per cell division sufficient to establish and preserve even unselected RNA3 derivatives in rapidly dividing yeast populations. Subgenomic mRNA synthesis provided a BMV-specific expression pathway for reporter gene-based measurement or genetic selection of BMV RNA-dependent RNA synthesis. Plasmids expressing B3URA3 and B3CAT showed that phenotypically effective, BMV-dependent gene expression was efficiently inducible in 1a2a$^+$ yeast to levels over 500,000-fold greater than background expression in 1a2a$^-$ yeast. This approach eliminates the need to synthesize and transfect in vitro transcripts to initiate BMV RNA replication, stabilizes RNA replicons in long-term culture, and allows more diverse viral RNA derivatives to be studied. This includes RNA3 derivatives without a selectable marker gene, such as B3CAT or wild-type RNA3, and even RNA3 derivatives incapable of complete RNA replication, such as Δ5′B3CAT. This approach should facilitate many experiments, including the isolation of yeast mutants affecting BMV RNA replication and gene expression. Below we discuss factors that influence BMV RNA replication or gene expression and BMV-independent background expression.

3′ effects on BMV RNA replication. The potential to initiate BMV RNA replication from DNA in vivo was first illustrated by Mori et al., who showed that BMV cDNAs fused to the cauliflower mosaic virus 35S promoter and polyadenylation signal induced local lesion infections in the plant *Chenopodium hybridum* (43). However, these plasmids were not infectious to the normal systemic host of BMV, barley, and initiated *Chenopodium* local lesions at a 1,000- to 10,000-fold-lower efficiency than in vitro transcripts from BMV cDNAs. One possible reason for this low efficiency was the absence of a mechanism to generate authentic viral 3′ ends. In the system described here, self-cleavage near the 3′ end of RNA3 was important to efficiently initiate RNA replication. Ribozymes positioned to give 0- or 3-nt 3′ extensions were both effective and nearly indistinguishable in supporting high-level CAT expression from B3CAT plasmids (Fig. 5 and 6), sufficient *URA3* expression from B3URA3 plasmids for uracil-independent growth (Fig. 7), and launching of B3URA3 as a free RNA replicon (Fig. 7C). By comparison, a 19-nt 3′ extension led to 50-fold-lower CAT expression, insufficient *URA3* expression for uracil-independent growth, and greatly reduced launching of B3URA3 as a free RNA replicon.

These results suggest that the in vivo transcripts with 19-nt 3′ extensions may be poorer templates for negative-strand RNA synthesis than correctly terminated (+0-nt) or +3-nt tran-

scripts. This is consistent with the finding of Miller et al. that 15- but not 6-nt 3′ extensions on RNA3 inhibit negative-strand RNA initiation in a BMV RNA-dependent RNA polymerase extract from infected barley (41). Similarly, Dzianott and Bujarski found that 3′ extensions 42 nt or longer inhibited the infectivity of BMV in vitro transcripts mechanically inoculated onto barley plants (17). However, in the same tests, the ribozyme-generated 19-nt extension used did not inhibit infectivity. The reason for the lower sensitivity of mechanically inoculated plants to the 19-nt extension is not clear. Given the negative-strand RNA initiation results of Miller et al., one possibility is that the template activity of +19-nt transcripts in plants and yeast may depend on removing at least part of the 3′ extension. Mechanical inoculation of leaves with abrasives causes extensive cell damage, which may increase exposure of in vitro transcripts to exo- or endonucleases able to trim the 19-nt 3′ extension. In vivo-synthesized transcripts in undamaged yeast cells may be exposed to fewer or different nucleases, yielding lower but still measurable template activity for +19-nt transcripts.

While +19-nt transcripts do not appear to be efficient templates for initiating BMV RNA synthesis, they may interact with some factors involved in RNA synthesis and competitively interfere with other templates. When plated on glucose medium without uracil, galactose-grown 1a2a$^+$ yeast with pB3URA3+19(A) gave rise to a few colonies in which independent, RNA-based replication of the B3URA3 RNA replicon had been initiated (Fig. 7C, row 1). When the same yeast was plated onto galactose medium without uracil (Fig. 7A, row 1), no colonies appeared, implying that continued transcription of B3URA3 RNA with the 19-nt extension inhibited replication of authentic B3URA3 RNA. No analogous interference was seen with continued transcription of pB3URA3(A) or pB3URA3+3(A) (Fig. 7A and C, rows 3 and 5).

5′ effects and initiation of BMV RNA replication. The ability to strongly induce or repress the *GAL1* promoter by changing the carbon source was very useful in the experiments reported here. Although the *GAL1* promoter produced multiple transcription starts (33), BMV RNA replication selectively amplified RNA3 with the authentic viral 5′ end (Fig. 4). Transcripts with two or three extra 5′ nucleotides sometimes also appeared to be amplified to a much lesser extent and may have participated in initiating replication but lost extra 5′ bases in subsequent rounds of replication. While the relative contributions of different transcripts to initiating RNA replication remain uncertain, it may be possible to increase cDNA activity by further tailoring the promoter linkage to increase the fraction of primary transcripts with authentic viral 5′ ends. However, initial attempts to fuse the *GAL1* promoter more closely to the start of RNA3 resulted in clones with less biological activity. More work will be needed to assess the potential for improved promoter linkages and the effect of altered sequence junctions on the transcript initiation pattern.

Low background expression of marker genes and poly(A) effects. Applying yeast genetics to BMV RNA replication requires BMV-dependent yeast phenotypes that are selectable or screenable at the colony level. For DNA-initiated RNA replication, this required both that a gene inserted in RNA3 cDNA be expressed to phenotypically scoreable levels by BMV-specific pathways and that BMV-independent background expression be too low to confer a phenotype. In the present study, insertion of marker genes downstream of the BMV subgenomic mRNA promoter proved remarkably successful at making DNA-initiated gene expression dependent on BMV RNA synthesis. In addition to providing a strong, BMV-specific expression pathway, this positioning prevented marker gene translation directly from *GAL1*-promoted transcripts (see the introduction). Other sources of BMV-independent background expression (fortuitous promoters near the marker gene and RNA splicing, etc.) were also negligible for most experimental purposes (2,000- to 500,000-fold below expression by effective BMV replicons [Fig. 5]). Nevertheless, sensitive measurement of background expression revealed some potentially useful points.

Background expression levels under glucose repression of the *GAL1* promoter were independent of 1a and 2a (Fig. 5), implying that background expression resulted primarily from direct translation of low-level transcripts lacking one or more *cis*-acting signals required to produce BMV subgenomic mRNA. Given the apparent lack of splicing in *GAL1*-promoted transcripts, the simplest potential origin for such directly translatable transcripts appears to be the possible presence of one or more weak, fortuitous start sites for DNA-dependent transcription in RNA3 cDNA near the start of RNA4, downstream of signals for BMV subgenomic mRNA synthesis. The AT-rich sequence immediately upstream of the RNA4 start site may facilitate transcription initiation (4). The consistent, approximately 10-fold reduction in background expression in galactose-grown 1a2a$^-$ yeast relative to glucose-grown 1a2a$^-$ or 1a2a$^+$ yeast (Fig. 5) suggests that initiation at such cryptic promoters might be inhibited by strong, galactose-induced transcription from the upstream *GAL1* promoter.

For pB3CAT(A) and pB3CAT+3(A) relative to pB3CAT and pB3CAT+3, addition of a polyadenylation signal downstream of RNA3 cDNA increased 1a- and 2a-independent background CAT expression 40- to 50-fold in glucose and 5- to 10-fold in galactose (Fig. 5). Though still negligible compared to BMV-directed CAT expression, this increased background could reflect a role of poly(A) in nuclear export, translation, and/or stability of one or more contributing transcripts (15, 18, 30). Background CAT expression increased despite the presence of a self-cleaving ribozyme between the CAT gene and polyadenylation site. Particularly for pB3CAT+3(A), for which uncleaved transcripts did not detectably accumulate (Fig. 6A), this suggests that transient association of poly(A) with a transcript may be sufficient to affect its nuclear export and/or later expression. Further information on the in vivo kinetics and intracellular site of ribozyme cleavage may be helpful in clarifying these effects.

Despite its effect on BMV-independent background expression, the polyadenylation signal had no significant effect on the ability of the B3CAT plasmids to initiate BMV-dependent RNA replication (Fig. 6) and gene expression (Fig. 5). This might reflect a low threshold requirement for RNA3 transcripts to initiate the self-amplifying RNA replication process, the dependence of initial RNA replication on self-cleaved transcripts that have lost their poly(A) tails, or the possibility that poly(A)-dependent mRNA export from the nucleus is directly linked to polysome formation and translation (12), which could inhibit the use of RNA3 transcripts in replication.

ACKNOWLEDGMENTS

We thank Jozef Bujarski and L. A. Ball for generously providing pB3-17-self and p(δ0,0δ), respectively; Christopher Yu for technical assistance; Michael Culbertson, Elizabeth Craig, and their colleagues for helpful advice; and Satoshi Naito for encouragement throughout this work.

This research was supported by the National Institutes of Health under Public Health Service grants GM51301 and GM35072.

REFERENCES

1. **Ahlquist, P.** 1992. Bromovirus RNA replication and transcription. Curr. Opin. Genet. Dev. **2:**71–76.

2. **Ahlquist, P., R. French, M. Janda, and L. S. Loesch-Fries.** 1984. Multicomponent RNA plant virus infection derived from cloned viral cDNA. Proc. Natl. Acad. Sci. USA **81:**7066–7070.
3. **Ahlquist, P., and M. Janda.** 1984. cDNA cloning and in vitro transcription of the complete brome mosaic virus genome. Mol. Cell. Biol. **4:**2876–2882.
4. **Ahlquist, P., V. Luckow, and P. Kaesberg.** 1981. Complete nucleotide sequence of brome mosaic virus RNA3. J. Mol. Biol. **153:**23–38.
5. **Ahlquist, P., E. G. Strauss, C. M. Rice, J. H. Strauss, J. Haseloff, and D. Zimmern.** 1985. Sindbis virus proteins nsP1 and nsP2 contain homology to nonstructural proteins from several RNA plant viruses. J. Virol. **53:**536–542.
6. **Allison, R. F., M. Janda, and P. Ahlquist.** 1988. Infectious in vitro transcripts from cowpea chlorotic mottle virus cDNA clones and exchange of individual RNA components with brome mosaic virus. J. Virol. **62:**3581–3588.
7. **Allison, R. F., C. Thompson, and P. Ahlquist.** 1990. Regeneration of a functional RNA virus genome by recombination between deletion mutants and requirement for cowpea chlorotic mottle virus 3a and coat genes for systemic infection. Proc. Natl. Acad. Sci. USA **87:**1820–1824.
8. **Ammer, G.** 1983. Expression of genes in yeast using the *ADC1* promoter. Methods Enzymol. **101:**192–201.
9. **Ausubel, F. M., R. Brent, R. E. Kingston, D. D. Moore, J. G. Seidman, J. A. Smith, and K. Struhl (ed.).** 1989. Current protocols in molecular biology. John Wiley & Sons, New York, N.Y.
10. **Ball, L. A.** 1994. Replication of the genomic RNA of a positive-strand RNA animal virus from negative-sense transcripts. Proc. Natl. Acad. Sci. USA **91:**12443–12447.
11. **Been, M. D.** 1994. *Cis*- and *trans*-acting ribozymes from a human pathogen, hepatitis delta virus. Trends Biochem. Sci. **19:**251–256.
12. **Belgrader, P., J. Cheng, and L. E. Maquat.** 1993. Evidence to implicate translation by ribosomes in the mechanism by which nonsense codons reduce the nuclear level of human triosephosphate isomerase mRNA. Proc. Natl. Acad. Sci. USA **90:**482–486.
13. **Boyer, J.-C., and A. L. Haenni.** 1994. Infectious transcripts and cDNA clones of RNA viruses. Virology **198:**415–426.
14. **Bradford, M. M.** 1976. A rapid and sensitive method for the quantitation of microgram quantities of protein utilizing the principle of protein-dye binding. Anal. Biochem. **72:**248–254.
15. **Caponigro, G., and R. Parker.** 1996. Mechanisms and control of mRNA turnover in *Saccharomyces cerevisiae*. Microbiol. Rev. **60:**233–249.
16. **De Jong, W., and P. Ahlquist.** 1992. A hybrid plant RNA virus made by transferring the noncapsid movement protein from a rod-shaped to an icosahedral virus is competent for systemic infection. Proc. Natl. Acad. Sci. USA **89:**6808–6812.
17. **Dzianott, A. M., and J. J. Bujarski.** 1989. Derivation of an infectious viral RNA by autolytic cleavage of *in vitro* transcribed viral cDNAs. Proc. Natl. Acad. Sci. USA **86:**4823–4827.
18. **Eckner, R., W. Ellmeier, and M. L. Birnstiel.** 1991. Mature mRNA 3′ end formation stimulates RNA export from the nucleus. EMBO J. **10:**3513–3522.
19. **French, R., and P. Ahlquist.** 1987. Intercistronic as well as terminal sequences are required for efficient amplification of brome mosaic virus RNA3. J. Virol. **61:**1457–1465.
20. **French, R., and P. Ahlquist.** 1988. Characterization and engineering of sequences controlling in vivo synthesis of brome mosaic virus subgenomic RNA. J. Virol. **62:**2411–2420.
21. **French, R., M. Janda, and P. Ahlquist.** 1986. Bacterial gene inserted in an engineered RNA virus: efficient expression in monocotyledonous plant cells. Science **231:**1294–1297.
22. **Gietz, R. D., and A. Sugino.** 1988. New yeast-*Escherichia coli* shuttle vectors constructed with *in vitro* mutagenized yeast genes lacking six-base pair restriction sites. Gene **74:**527–534.
23. **Gupta, K., and D. Kingsbury.** 1984. Complete sequences of the intergenic and mRNA start signals in the Sendai virus genome: homologies with the genome of vesicular stomatitis virus. Nucleic Acids Res. **12:**3829–3841.
24. **Haseloff, J., and W. L. Gerlach.** 1988. Simple RNA enzymes with new and highly specific endonuclease activities. Nature **334:**585–591.
25. **Haseloff, J., P. Goelet, D. Zimmern, P. Ahlquist, R. Dasgupta, and P. Kaesberg.** 1984. Striking similarities in amino acid sequence among nonstructural proteins encoded by RNA viruses that have dissimilar genomic organization. Proc. Natl. Acad. Sci. USA **81:**4358–4362.
26. **Huang, Y., and G. G. Carmichael.** 1996. Role of polyadenylation in nucleocytoplasmic transport of mRNA. Mol. Cell. Biol. **16:**1534–1542.
27. **Ishikawa, M., and P. Ahlquist.** Unpublished data.
28. **Ishikawa, M., P. Kroner, P. Ahlquist, and T. Meshi.** 1991. Biological activities of hybrid RNAs generated by 3′-end exchanges between tobacco mosaic and brome mosaic viruses. J. Virol. **65:**3451–3459.
29. **Ito, H., Y. Fukuda, K. Murata, and A. Kimura.** 1983. Transformation of intact yeast cells treated with alkali cations. J. Bacteriol. **153:**163–168.
30. **Jackson, R. J., and N. Standart.** 1990. Do the poly(A) tail and 3′ untranslated region control mRNA translation? Cell **62:**15–24.
31. **Janda, M., and P. Ahlquist.** 1993. RNA-dependent replication, transcription, and persistence of brome mosaic virus RNA replicons in *S. cerevisiae*. Cell **72:**961–970.
32. **Janda, M., R. French, and P. Ahlquist.** 1987. High efficiency T7 polymerase synthesis of infectious RNA from cloned brome mosaic virus cDNA and effects of 5′ extensions on transcript infectivity. Virology **158:**259–262.
33. **Johnston, M., and R. W. Davis.** 1984. Sequences that regulate the divergent *GAL1-GAL10* promoter in *Saccharomyces cerevisiae*. Mol. Cell. Biol. **4:**1440–1448.
34. **Johnston, M.** 1987. A model fungal gene regulatory mechanism: the *GAL* genes of *Saccharomyces cerevisiae*. Microbiol. Rev. **51:**458–476.
35. **Kao, C. C., and P. Ahlquist.** 1992. Identification of the domains required for direct interaction of the helicase-like and polymerase-like RNA replication proteins of brome mosaic virus. J. Virol. **66:**7293–7302.
36. **Kao, C. C., R. Quadt, R. P. Hershberger, and P. Ahlquist.** 1992. Brome mosaic virus RNA replication proteins 1a and 2a form a complex in vitro. J. Virol. **66:**6322–6329.
37. **Kiberstis, P. A., L. S. Loesch-Fries, and T. C. Hall.** 1981. Viral protein synthesis in barley protoplasts inoculated with native and fractionated brome mosaic virus RNA. Virology **112:**804–808.
38. **Kroner, P. A., B. M. Young, and P. Ahlquist.** 1990. Analysis of the role of brome mosaic virus 1a protein domains in RNA replication, using linker insertion mutagenesis. J. Virol. **64:**6110–6120.
39. **Kunkel, T. A., J. D. Roberts, and R. A. Zakour.** 1987. Rapid and efficient site-specific mutagenesis without phenotypic selection. Methods Enzymol. **154:**367–382.
40. **Lai, M. M. C.** 1992. RNA recombination in animal and plant viruses. Microbiol. Rev. **56:**61–79.
41. **Miller, W. A., J. J. Bujarski, T. W. Dreher, and T. C. Hall.** 1986. Minus-strand initiation by brome mosaic virus replicase within the 3′ tRNA-like structure of native and modified RNA templates. J. Mol. Biol. **187:**537–546.
42. **Mise, K., and P. Ahlquist.** 1995. Host specificity restriction by bromovirus cell-to-cell movement protein occurs after initial cell-to-cell spread of infection in nonhost plants. Virology **206:**276–286.
43. **Mori, M., K. Mise, K. Kobayashi, T. Okuno, and I. Furusawa.** 1991. Infectivity of plasmids containing brome mosaic virus cDNA linked to the cauliflower mosaic virus 35S RNA promoter. J. Gen. Virol. **72:**243–246.
44. **Pogue, G. P., and T. C. Hall.** 1992. The requirement for a 5′ stem-loop structure in brome mosaic virus replication supports a new model for viral positive-strand RNA initiation. J. Virol. **66:**674–684.
45. **Quadt, R., M. Ishikawa, M. Janda, and P. Ahlquist.** 1995. Formation of brome mosaic virus RNA-dependent RNA polymerase in yeast requires coexpression of viral proteins and viral RNA. Proc. Natl. Acad. Sci. USA **92:**4892–4896.
46. **Quadt, R., and E. M. J. Jaspars.** 1990. Purification and characterization of brome mosaic virus RNA-dependent RNA polymerase. Virology **178:**189–194.
47. **Quadt, R., C. C. Kao, K. S. Browning, R. P. Hershberger, and P. Ahlquist.** 1993. Characterization of a host protein associated with brome mosaic virus RNA-dependent RNA polymerase. Proc. Natl. Acad. Sci. USA **90:**1498–1502.
48. **Rao, A. L. N., and T. C. Hall.** 1993. Recombination and polymerase error facilitate restoration of infectivity in brome mosaic virus. J. Virol. **67:**969–979.
49. **Restrepo-Hartwig, M. A., and P. Ahlquist.** 1996. Brome mosaic virus helicase- and polymerase-like proteins colocalize on the endoplasmic reticulum at sites of viral RNA synthesis. J. Virol. **70:**8908–8916.
50. **Rose, M., and F. Winston.** 1984. Identification of a Ty insertion within the coding sequence of the *S. cerevisiae URA3* gene. Mol. Gen. Genet. **193:**557–560.
51. **Sacher, R., and P. Ahlquist.** 1989. Effects of deletions in the N-terminal basic arm of brome mosaic virus coat protein on RNA packaging and systemic infection. J. Virol. **63:**4545–4552.
52. **Sachs, A. B., and R. W. Davis.** 1989. The poly(A) binding protein is required for poly(A) shortening and 60S ribosomal subunit-dependent translation initiation. Cell **58:**857–867.
53. **Steinhauer, D. A., and J. J. Holland.** 1987. Rapid evolution of RNA viruses. Annu. Rev. Microbiol. **41:**409–433.